Platination of the $(T_2G_4)_4$ Telomeric Sequence: A Structural and Cross-Linking Study†

Sophie Redon, Sophie Bombard, Miguel-Angel Elizondo-Riojas,‡ and Jean-Claude Chottard*

Laboratoire de Chimie et Biochimie Pharmacologiques et Toxicologiques, UMR 8601 CNRS, Université Paris V, 45 Rue des Saints-Pères, 75270 Paris Cedex 06, France

Received July 6, 2000; Revised Manuscript Received April 9, 2001

ABSTRACT: The telomeric sequence $(T_2G_4)_4$ was platinated in aqueous solutions containing 50 mM $LiClO_4$, $NaClO_4$, or $KClO_4$. The identification of the guanines which reacted with $[Pt(NH_3)_3(H_2O)]^{2+}$ revealed that the same type of folding exists in the presence of the three cations and that the latter determine the relative stabilities of the G-quadruplex structures in the order $K^+ > Na^+ \gg Li^+$. The tri-ammine complex yielded ca. 40−90% of adducts, mono- and poly-platinated, bound to 4 guanines out of the 16 guanines in the sequence, in the decreasing amounts G9 > G15 ≫ G3 > G21. The formation of these adducts was interpreted with a G-quadruplex structure obtained by restrained molecular dynamics (rMD) simulations which confirms the schematic model proposed by Williamson et al. [(1989) *Cell 59*, 871−880]. The bifunctional complexes *cis*- and *trans*-$[Pt(NH_3)_2(H_2O)_2]^{2+}$ also first reacted with G9 and G15 and gave cross-linked adducts between two guanines, which did not exceed 5% each of the products formed. Both the cis and trans isomers formed a G3-G15 platinum chelate, and the second also formed bis-chelates at both ends of the G-quadruplex structure: G3-G15/G9-G21 and G3-G15/G9-G24. The rMD simulations showed that the cross-linking reactions by the trans complex can occur without disturbing the stacking of the three G-quartets.

Several G-rich sequences such as telomeres (*1*), immunoglobin switch region (*2*), fragile X (*3*), or the *c-myc* promoter (*4*) are present in the genome. In vitro, G-rich oligonucleotides in the single-stranded form can adopt, in the presence of sodium or potassium ions, highly stable structures called G-quadruplexes. They result from the stacking of planar quartets of guanines, the latter being associated to each other by Hoogsteen-type hydrogen bonds involving their four N7 atoms (*5*). The sodium and potassium ions appear to stabilize the stacking through their interactions with the carbonyl oxygens of the eight guanines of two adjacent quartets (*6*). Several types of G-quadruplex structures have been characterized depending on the sequences containing the G-tracks and the nature and concentration of the monovalent cation. They are classified according to the number of strands involved, to the syn or anti conformation of the guanines, and to the relative parallel- or antiparallel-type orientations of the strands or parts of the sequence in the folding (*7*). The structures were determined by chemical analyses and in some cases by NMR[1] and X-ray crystallography. Single-stranded sequences containing at least four repeats of three or four guanines fold into intramolecular G-quadruplex structures (*5, 7*). This is the case for the $(T_2G_4)_4$ telomeric sequence studied in this work.

The occurrence of G-quadruplex structures in vivo has been considered but lacks experimental evidence at present. It has been postulated that such structures might regulate gene expression. The telomeres, which are constituted of G-rich repeat sequences located at the ends of eukaryotic chromosomes and particularly in the 3′-terminal single-strand, are essential for preventing aberrant recombination and degradation of DNA (*1*). At each division of somatic cells, telomeres are shortened, a process leading to senescence and death (*8, 9*). This can be compensated by the synthesis of the repeat sequences at the 3′-end of the chromosomes by the ribonucleoprotein telomerase. Such an activity might be involved in the immortalization of tumor cells (*10*). It has been shown in vitro, that G-quadruplex structures of the human sequence $(T_2AG_3)_4$ formed in the presence of Na^+ or K^+ ions (*11, 12*) or of molecules stabilizing the G-quartet stacks, like anthraquinones (*13*−*15*) or porphyrins (*16*), inhibit the activity of telomerase. Telomeres and telomerase therefore appear as potential targets for anticancer chemotherapy (*17, 18*). The antitumor drug cisplatin, known for its high affinity for GG sequences, was found to inhibit telomerase activity in testicular cancer cells (*19*) and to reduce telomere length in treated cells (*20*).

Platinum complexes bind covalently to nucleobases and especially to the N7 atom of guanines (*21*). The four guanines of a G-quartet have their N7 atoms involved in hydrogen bonding. Therefore, within a G-quadruplex structure, only the guanines out of the stack of G-quartets should react with

† This work was supported by La Ligue Nationale Française contre le Cancer and l'Association pour la Recherche sur le Cancer (Contrat 9799).

* Corresponding author. Phone: 33 (0)142862168. Fax: 33 (0)1 42868387. E-mail: Jean-Claude.Chottard@biomedicale.univ-paris5.fr.

‡ On leave from the Centro Universitario Contra el Cancer (CUCC), Hospital Universitario "Dr. José Eleuterio Gonzalez", Universidad Autonoma de Nuevo Leon, Monterrey, N.L., Mexico.

[1] Abbreviations: NMR, nuclear magnetic resonance; rMD, restrained molecular dynamics; ATP, adenosine triphosphate; EDTA, ethylenediaminetetraacetic acid; DMS, dimethyl sulfate.

10.1021/bi001565a CCC: $20.00
Published on Web 06/28/2001

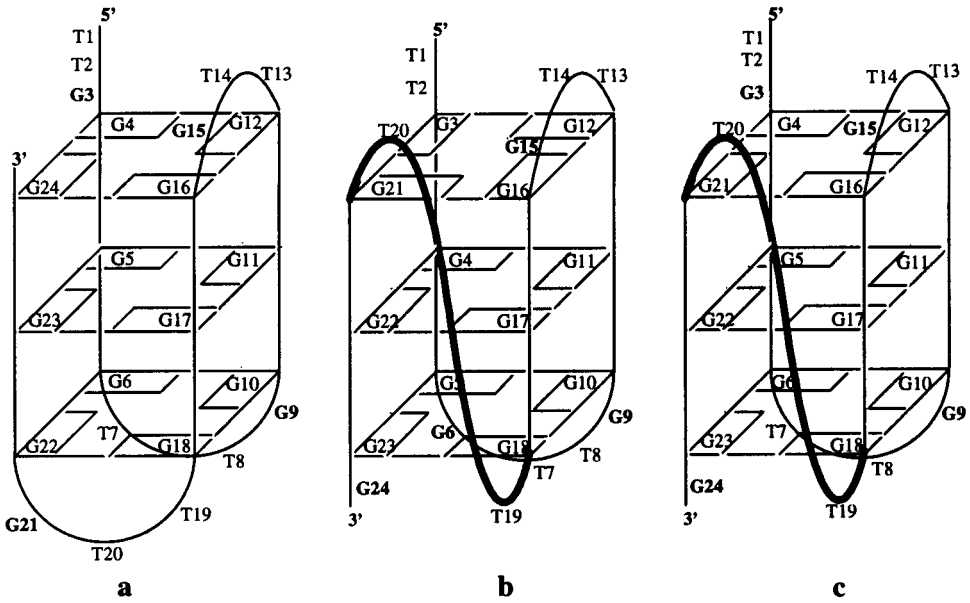

FIGURE 1: Three schematic models of the folded structures of $(T_2G_4)_4$ in Na^+ solution: **a** proposed by Williamson et al. (*22*), **b** proposed by Wang and Patel (*24*) (atomic coordinates available for the corresponding structure **B** from the Brookhaven database), and **c** proposed in this work. In the text, we distinguish the schematic models **a**, **b**, and **c** from the corresponding calculated structures **A**, **B**, and **C**.

electrophilic species such as platinum(II) complexes. We wondered if the monofunctional $[PtCl(NH_3)_3]Cl$ complex, in its aqua form, could be used as a probe for these structures and if the bifunctional platinum complexes, *cis*-$[PtCl_2(NH_3)_2]$ and *trans*-$[PtCl_2(NH_3)_2]$ in their aqua forms, could cross-link accessible guanines of these G-quadruplex structures. Apart from structural information, such cross-linking might lead to telomerase inhibition.

We first chose the telomeric sequence of *Tetrahymena* $(T_2G_4)_4$ for which two models of G-quadruplex had been proposed in Na^+-containing solution. One was deduced from photochemical cross-linking, inosine−guanosine substitution, and dimethyl sulfate G-N7 methylation experiments: **a**[2] (*22*, *23*); the other from NMR studies: **b** (*24*). The two models **a** and **b** (Figure 1) differ by the geometries of their loops and by the guanines involved in the G-quartets.

This paper reports the analysis of the platination sites of $(T_2G_4)_4$ after reaction with $[Pt(NH_3)_3(H_2O)]^{2+}$ (**1**) in the presence of the different structuring cations, Li^+, Na^+, and K^+. The data are discussed in relation with possible G-quadruplex structures for $(T_2G_4)_4$. It also shows that the bifunctional *cis*- and *trans*-$[Pt(NH_3)_2(H_2O)_2]^{2+}$ complexes **2** and **3** can cross-link the G-quadruplex structures depending on the folding conditions and on the ability of each complex to span nonadjacent guanines. The platination and cross-linking data are interpreted using the G-quadruplex structures obtained from restrained molecular dynamics simulations.

EXPERIMENTAL PROCEDURES

Materials. $(T_2G_4)_4$ and the length markers 8-mer, 11-mer, 16-mer, 20-mer, and 33-mer were synthesized by the phosphoramidite method in the laboratory of Dr. T. Huynh Dinh (Institut Pasteur, Paris), purified by 15% denaturing gel electrophoresis and located by UV-shadowing. After elution and ethanol precipitation, they were desalted on a Sephadex G50 column and stored at −20 °C in 1 mM aqueous solution. T4 polynucleotide kinase and [γ-^{32}P]ATP were from Pharmacia Biotech, NaCN was from Merck, and dimethyl sulfate (DMS) and piperidine were from Sigma. *cis*-$[PtCl_2(NH_3)_2]$ and *trans*-$[PtCl_2(NH_3)_2]$ were kindly provided by Johnson Matthey (London, United Kingdom). *cis*-$[Pt(NH_3)_2(H_2O)_2]^{2+}$ and *trans*-$[Pt(NH_3)_2(H_2O)_2]^{2+}$ were prepared by dissolving a suspension of *cis*-$[Pt(NO_3)_2(NH_3)_2]$ and *trans*-$[Pt(NO_3)_2(NH_3)_2]$ in water, respectively, formed by reaction of *cis*-$[PtCl_2(NH_3)_2]$ and *trans*-$[PtCl_2(NH_3)_2]$ with silver nitrate (*25*). $[Pt(NH_3)_3(H_2O)]^{2+}$ was prepared from $[PtCl(NH_3)_3](NO_3)$ (*25*).

5′-End-Labeling Reactions. $(T_2G_4)_4$ and the 8-mer, 11-mer, 16-mer, 20-mer, and 33-mer were 5′-end-labeled using polynucleotide kinase and [γ-^{32}P]ATP. The reaction products were purified on 20% denaturing gel electrophoresis without EDTA or on a Sephadex G50 column.

Nondenaturing Gel Electrophoresis. Nondenaturing gel electrophoresis of $(T_2G_4)_4$ (0.5−4 μM) was performed as previously described (*22*) with some modifications: 12% polyacrylamide gels (29:1 acrylamide:bisacrylamide ratio) containing tris(hydroxymethyl)aminomethane−borate without EDTA (0.088 M Tris−borate, pH 8.3) in 50 mM LiCl, NaCl, or KCl at 4 °C. The gels were run at 120 V until the bromophenol blue marker migrated 18 cm (20 h). Figure 1S (Supporting Information) first shows that in the presence of any of the cations, Li^+, Na^+, and K^+, $(T_2G_4)_4$ adopts structures which migrate faster than a nonfolded 24-mer. For the three cations, the bands observed were concentration-independent. In the presence of Li^+ and Na^+, only one spot was observed with a faster migration for Na^+. In the presence of K^+, three spots appeared accounting, respectively, in the migration order for 52, 44, and 4% of the total radioactivity. To understand the significance of these three spots, we eluted the corresponding compounds from the gel, with 50 mM KCl, followed by ethanol precipitation. After incubation in 50 mM KCl, the product from each spot was submitted to

[2] In the text and figures, **a** (**b**,**c**) correspond to schematic representations of quadruplex structures of $(T_2G_4)_4$ and **A** (**B**,**C**) to the corresponding structures simulated by rMD calculations.

nondenaturing gel migration. The product from the first spot (52% in the initial mixture) gave a single spot identical to the former one. The product from the second spot (initially 44%) gave the two major spots, showing that it undergoes a transformation into the major form of $(T_2G_4)_4$ in K^+ solution. The product from the minor spot remained unchanged. Despite its migration similar to that of an unfolded 24-mer, this compound is not the unfolded form of $(T_2G_4)_4$ because it would have given the two major spots. It could be the stable hairpin dimer G-quadruplex previously proposed by Hardin et al. (*26*). Such a "48-mer" quadruplex could migrate as a 24-mer. Our nondenaturing gel data, with each isolated compound, do not support an equilibrium between the two major forms, because only the second one is transformed into the first, whereas their initial proportions in the mixture were relatively close. They suggest that the formation of quadruplex structures could involve several steps able to give different folded forms depending on the cation and susceptible to rearrange into the most stable one(s).

Platination of $(T_2G_4)_4$ in the Presence of Li^+, Na^+, or K^+. 5′-End-radiolabeled $(T_2G_4)_4$ mixed either with 100 or with 0.4 μM nonradiolabeled material was incubated in both cases with 300 μM of the platinum complex in respective 1:3 or 1:750 ratios of reactants. The reactions were run for 2 h at 25 °C in 50 mM $LiClO_4$, $NaClO_4$, or $KClO_4$ with $[Pt(NH_3)_3(H_2O)](NO_3)_2$ (**1**), *cis*-$[Pt(NH_3)_2(H_2O)_2](NO_3)_2$ (**2**), or *trans*-$[Pt(NH_3)_2(H_2O)_2](NO_3)_2$ (**3**). With **3**, the platination was also run for 24 h. For the experiments with a very large excess of complex (750:1), the latter was removed after 2 h by ethanol precipitation, and with **3** a further 24 h incubation was used to allow chelation of the monoadducts.

Because of the existence of two different forms of $(T_2G_4)_4$ in the presence of K^+, the compounds from the two major spots on the gel (vide supra) were reacted indepedently with the three platinum complexes (250 μM) during their elution in 250 μL of 50 mM $KClO_4$, for 2 h at 10 °C. After precipitation by ethanol and dissolution in 50 mM $KClO_4$, the adducts of **1** and **2** were analyzed, and those of **3** were first incubated for 24 h at 25 °C before analysis. The same adducts were obtained from the isolated compounds as those formed from the platination of $(T_2G_4)_4$ in 50 mM K^+.

The platinated oligonucleotides were separated by 20% polyacrylamide denaturing gel electrophoresis and located by autoradiography. They migrated differently according to their mass and charge.

Determination and Quantification of the Platinum Binding Sites. After elution from the gel and ethanol precipitation, the compounds from each band were treated with DMS−piperidine in Maxam−Gilbert sequencing conditions (*27*−*29*). The fragments were deplatinated by 2 M NaCN for 18 h at 37 °C and precipitated to allow a comparative gel electrophoresis analysis with nonplatinated $(T_2G_4)_4$. The various spots were quantified using a Dynamic Molecular Phosphorimager with the Imagequant software for data processing. As N7-platinated guanines are no longer reactive with dimethyl sulfate (DMS), the sites and amounts of platination could be deduced from the absence or smaller intensity of the spots corresponding to the cleavable guanosines. We compared for each guanine, in exactly identical conditions, the percentage of DMS−piperidine cleavage for the nonplatinated and the platinated oligonucleotides. For each guanine, the ratio: [(% cleavage of nonplatinated $(T_2G_4)_4$) − (% cleavage of platinated $(T_2G_4)_4$)]/(% cleavage of nonplatinated $(T_2G_4)_4$) was used to define its *percentage of platination*. For a mixture of comigrating oligonucleotides platinated differently, the percentage of platination of one guanine is 100% only if its adduct is present in all the products. The maximal experimental error was evaluated to 15%, limiting the analysis of the minor adducts.

In Vacuo Restrained Molecular Dynamics Simulations. All energy minimization and restrained molecular dynamics calculations were performed on a Silicon Graphics OCTANE workstation using the Amber 4.1 package (*30*), with the force field "parm98.dat" (*31*), complemented with force field parameters for platinum binding as described previously (*32*). The four improper torsion angles terms used to parametrize the bending of the Pt−N7 bonds out of the guanine planes (*32*) were reduced according to Chval and Síp (*33*) in order to account for guanine puckering. For the platination reactions, the atomic charges and distances for the $[Pt(NH_3)_2(Guo)_2(H_2O)]^{2+}$ pentacoordinated moieties were derived from density functional theory calculation on the 9-methylguanine derivatives *cis*- and *trans*-$[Pt(NH_3)_2(9\text{-Me-Guo})_2]^{2+}$, employing the B3LYP hybrid functional implemented in Gaussian94 (*34*); the LANL2DZ pseudopotential/pseudoorbital basis set was used for Pt, and all-electron basis 3-21G* was used for the other atoms. The atomic charges were determined from fits to the electrostatic potentials using the Merz−Kollman routine (*35*); charges of chemically identical atoms were averaged.

The Na^+ folded form of $(T_2G_4)_4$ was chosen for our calculations because it appeared as a single species on the nondenaturing gel and because it gave identified adducts with all three complexes **1**, **2**, and **3**. Moreover, the atomic coordinates of the three G-quartets of the $(T_2G_4)_4$ structure **B**, corresponding to model **b** (Figure 1) in the presence of Na^+, published by Wang et al. (*24*) were available from the Brookhaven database and were used as the starting point for all constructions. Model **c** was built to account for the G3-G15/G9-G24 bis-cross-linking of $(T_2G_4)_4$ by **3** (vide infra). Both structures **A** and **C** were derived from these initial structures by on-screen manipulations, using the Moil-View (*36*) and XmMol programs (*37*), combined with simulated annealing and energy minimization techniques using Amber 4.1 (*30*) (Figure 2 and Figure 2S in the Supporting Information). To start the calculations, 3 sodium ions were placed within the 3 G-quartets, whereas 20 additional Na^+ ions were positioned at a 6 Å distance from the phosphodiester oxygen atoms to neutralize the whole structure. To allow the cations to find the most favorable electrostatic positions, they were not restrained between 0 and 10 Å, but a parabolic distance restraint force of 25 kcal·mol^{-1}·Å^{-1} between 10 and 12 Å was applied. The electrostatic energy was evaluated using the distance-dependent dielectric function $\epsilon = 4r$ to mimic bulk solvent screening effects. To keep the G-quadruplex structure folding during the in vacuo simulation at 300 K, Hoogsteen hydrogen bonds were defined as distance restraints between donor and acceptor atoms. A total of 24 parabolic distance restraint forces (8 for each G-tetrad) of 25 kcal·mol^{-1}·Å^{-1} were applied between 1.95 and 2.25 Å and nothing for a smaller hydrogen bond distance. For longer distances, a linear restraint force with the slope of the parabola at 2.25 Å was applied; 18 Na^+, instead of 20 Na^+, were used to neutralize the structures bearing 1 dicationic

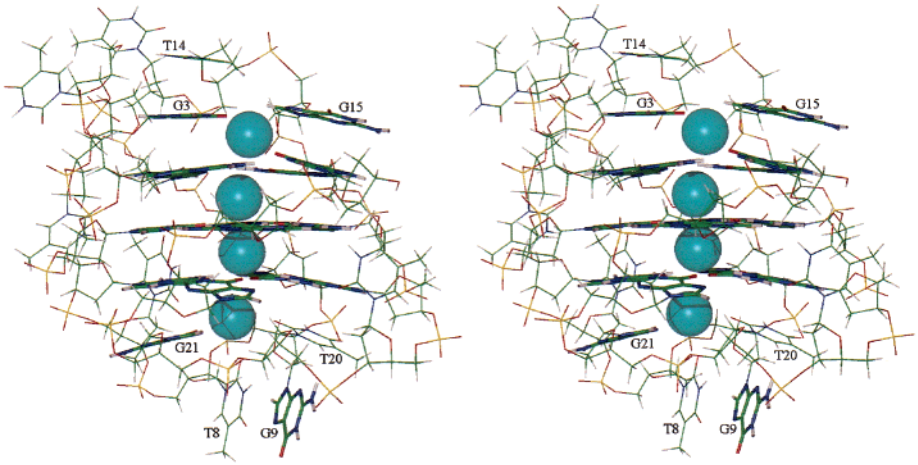

FIGURE 2: Stereoview of the energy-minimized folded structure **A** of $(T_2G_4)_4$ in Na^+ solution corresponding to the schematic model **a**. The guanine bases are represented in "stick" format, and the size of the Na^+ cation represents its van der Waals radius.

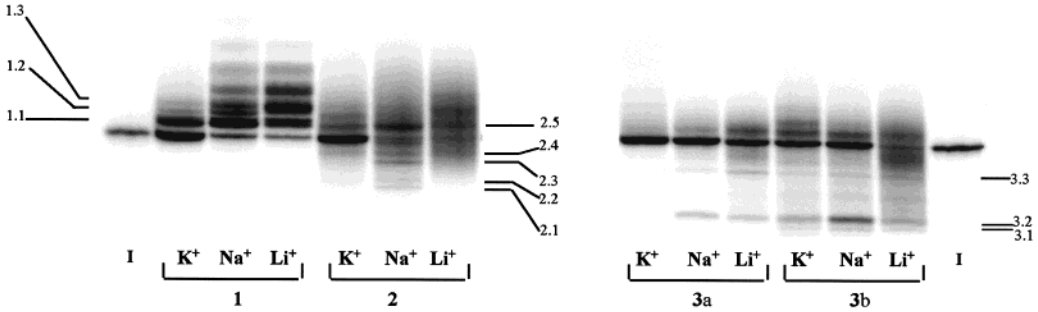

FIGURE 3: Denaturing gel electrophoresis (20% acrylamide) of the platination products of $(T_2G_4)_4$ in the presence of Li^+, Na^+, and K^+ by $[Pt(NH_3)_3(H_2O)]^{2+}$ **1**, *cis*-$[Pt(NH_3)_2(H_2O)_2]^{2+}$ **2**, and *trans*-$[Pt(NH_3)_2(H_2O)_2]^{2+}$ **3**. Lanes 1, 2, and 3 indicate the platinum complex used (for lane 3, a and b indicate 2 and 24 h reactions, respectively); lane I is $(T_2G_4)_4$; K^+, Na^+, and Li^+ indicate the cation in the medium.

platinum complex, and 16 Na^+ for structures with 2 platinum residues (Figures 5 and 6).

The rMD simulations of the pentacoordinated intermediates of several cross-linking reactions by complexes **2** and **3** were performed considering that the second guanine makes an axial attack on the square planar complex with a 90° G(N7)−Pt−G(N7) angle in the case of **2** and 120° in the case of **3** (*38*, *39*) (Figure 3S, Supporting Information). In the case of **2**, there are two possible enantiomeric pentacoordinated states which become diastereoisomeric when bound to the oligonucleotide. To take this into account, the force field of Amber 4.1 was complemented with unrestrained dihedral angles for the pentacoordinated state, to find the most stable diastereoisomer, during the rMD simulations.

The rMD simulations were performed with a time step of 1 fs and a cutoff distance of 9 Å. The structure was heated from 0 to 300 K in 5 ps; then a Maxwellian distribution of velocities with different initial random seed was applied, after which a 5 ps period was used to equilibrate the system and a second Maxwellian distribution of velocities was applied with a different initial random seed. Subsequently, a 250 ps dynamics simulation was performed, and every 50 ps one structure was selected for refinement, including simulated annealing (cooling to 0 K in 5 ps) and energy minimization. For the various cross-linking reactions studied, the lowest energy structures are shown in Figures 5 (**D**), 4S (**E**) (Supporting Information), and 6 (**F**). They were generated using the VMD program (*40*). The energy values must be considered with caution because the in vacuo restrained molecular dynamics simulations include solvating effects only implicitly. However, we can use these values to compare the steric and electrostatic stabilities of similar structures.

RESULTS

Platination of $(T_2G_4)_4$ in 50 mM Li^+, Na^+, or K^+ Perchlorate by Triammineaquaplatinum(II). The aim of this investigation was to identify which guanines are available to platination on the folded form(s) of $(T_2G_4)_4$ and to see if the previously proposed Na^+ models **a** and **b** could account for the data (Figure 1).

$[Pt(NH_3)_3(H_2O)](NO_3)_2$ (**1**) was reacted with $(T_2G_4)_4$ in a 3:1 platinum to oligonucleotide ratio. The platinated oligonucleotides have a slower migration than $(T_2G_4)_4$ and could be separated according to their number of $Pt(NH_3)_3^{2+}$ adducts. However, we could not always separate oligonucleotides with the same number of adducts bound in different positions. The extent of platination of $(T_2G_4)_4$ was 90, 80, and 40%, respectively, after 2 h of reaction in the presence of Li^+, Na^+, and K^+ (Figure 3). A decreasing number of bands is observed from Li^+ to K^+, suggesting less platination sites. The sequencing of the product of band 1.1 (Experimental Procedures and Figure 4) showed that it corresponded to 80% of the adduct on G9 in the presence of Na^+ and K^+ and 50% in Li^+. Therefore, band 1.1 contains monoadducts and essentially that on G9. The product of band 1.2 revealed

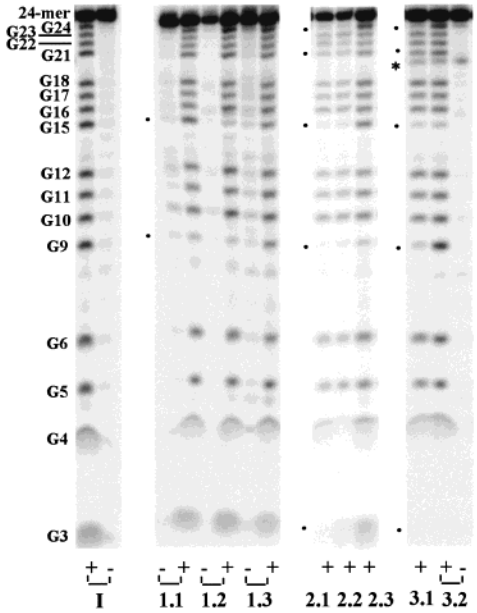

FIGURE 4: Analysis by sequencing gel electrophoresis of the platination products of $(T_2G_4)_4$ isolated from the bands of the denaturing gel of Figure 3. Lane I, $(T_2G_4)_4$; (+), DMS, piperidine followed by NaCN treatment; (−), piperidine alone followed by NaCN treatment. Lanes 1.*i*, 2.*i*, and 3.*i* refer to the platinum complex used and to the labeling of the bands in Figure 3. An uncompletely deplatinated product was still present after NaCN treatment of lanes 3.1 and 3.2, which migrate faster than G21 (*). The dots between the lanes (·) indicate the platinated sites revealed by the absence of cleavage.

diplatinated adducts accounting for 90% reaction on G9 and 85% on G15 in Na^+ and K^+, together with other guanines in Li^+. The products of band 1.3 and those having a slower migration corresponded to multiplatinated adducts involving essentially G3, G6, G9, G12, G15, and G21; in the presence of K^+, 50% platination is still observed on both G3 and G9. Experiments were run with a very large excess of platinum to oligonucleotide (750:1 ratio) in order to test the stability of the quadruplex structure versus unfolding. After 2 h reaction, no guanine was protected from platination in Li^+, and the four guanines of the central quartet remained protected in Na^+ whereas the four guanines G9, G15 and G3, G21 remained the only platinated bases in K^+, as in the case of the 3:1 ratio.

The G9-monoplatinated and G9, G15-diplatinated adducts of $(T_2G_4)_4$ exhibited on a K^+ nondenaturing gel a faster migration than that of the nonstructured 24-mer and comparable to that of its folded form.

Platination of $(T_2G_4)_4$ in 50 mM Li^+, Na^+, or K^+ Perchlorate by cis-Diamminediaquaplatinum(II). *cis*-$[Pt(NH_3)_2(H_2O)_2](NO_3)_2$ (**2**) was reacted with $(T_2G_4)_4$ in a 3:1 platinum to oligonucleotide ratio. The adducts were analyzed as above. After 2 h, only 30% of $(T_2G_4)_4$ had reacted in K^+ compared to 85% in Li^+ or Na^+. The major observation from Figure 3 is that complex mixtures of adducts were formed in the presence of the three cations and that only Na^+ gave analyzable distinct electrophoresis bands. Among these, band 2.5, with a slower migration than that of $(T_2G_4)_4$, contained a mixture of adducts which did not reveal any selective platination. Four bands (2.1−2.4) migrated faster than that of $(T_2G_4)_4$, accounting for 36% of the starting oligonucleotide.

The analysis of the faster migrating products revealed the following platinated sites (%), band 2.1: G9 (100), G15 (100), G3 (80), G24 (50), and G21 (40); band 2.2: G9 (100), G15 (90), G21 (25), and G24 (25); bands 2.3 and 2.4: G9 (80) together with smaller proportions on G3, G6, G12, G15, G21, and G22. A comparison of these band migrations to those of products obtained with complex **3** led us to conclude that the compounds of band 2.1 contain the G3-G15 chelate together with two monoadducts (vide infra). Therefore, in all cases, only multiplatinated adducts were characterized. No single cross-linked oligonucleotide was isolated.

Platination of $(T_2G_4)_4$ in 50 mM Li^+, Na^+, or K^+ Perchlorate by trans-Diamminediaquaplatinum(II). *trans*-$[Pt(NH_3)_2(H_2O)_2](NO_3)_2$ (**3**) required 24 h of reaction instead of 2 h for **1** and **2** to give oligonucleotide respective conversions of 85% in Li^+ and 40% in both Na^+ and K^+. In the three media, **3** gave adducts migrating either slower or faster than $(T_2G_4)_4$ on gel electrophoresis. No selective platination sites were identified for the slower migrating products.

The products of the three faster migrating bands (3.1−3.3, Figure 3) accounted for 15% of the total radioactivity. The product of band 3.2 was the simplest to analyze as it revealed 90% platination on G3 and 90% platination on G15, concluding in only one cross-linked adduct: the G3-G15 chelate of the *trans*-$Pt(NH_3)_2^{2+}$ moiety. It is notewortly that no product with a single G9-G21 or G9-G24 cross-link was detected. For band 3.1, the platination sites of the products (%) were the following: G3 (85), G9 (80), G15 (85), G21 (45), and G24 (45). These data can be interpreted by the presence of two or three platinums per oligonucleotide, corresponding either to the two G3-G15/G9-G21 or G3-G15/G9-G24 chelates or to two types of adducts including the G3-G15 chelate together with two monoadducts on G9 and G21 or G24. It is known that in identical conditions a compact DNA structure exhibits, on a denaturing gel, a faster migration than that expected according to its mass and charge (*41*). It has been shown that the photochemical formation of thymine dimers leads to a faster migration of the $(T_4G_4)_4$ and $(T_2G_4)_4$ oligonucleotides (*22*). In our case, band 3.1 migrates faster than band 3.2 which contains the single G3-G15 chelate. Therefore, with two platinums bound and an extra 2+ charge inducing gel retardation, the faster migrating compound of band 3.1 should be more compact than the singly G3-G15 cross-linked quadruplex. This strongly suggests that the compound of band 3.1 is a bis-cross-linked adduct, at each end of the quadruplex, rather than a three platinum adduct with only one cross-link. In the same line of reasoning, considering the platination by **2** (vide supra), band 2.1 migrated slower than bands 3.1 and 3.2 (the G3-G15 chelate) on the same gel, strongly suggesting that the products of 2.1 contain only one platinum cross-link together with two monoadducts.

In Vacuo Restrained Molecular Dynamics (rMD) Simulations. We first ran restrained molecular dynamics simulations of $(T_2G_4)_4$ in the presence of Na^+, based on the schematic model **a** (Figure 1) which had been previously proposed by Williamson et al. (*22*). We selected the lowest energy structure **A** (Figure 2) which presented two Na^+ intercalated between the three G-quartets and two others associated at each end of the quadruplex structure. Structure **A** suggests that G9 and G15 should be the most accessible to platination

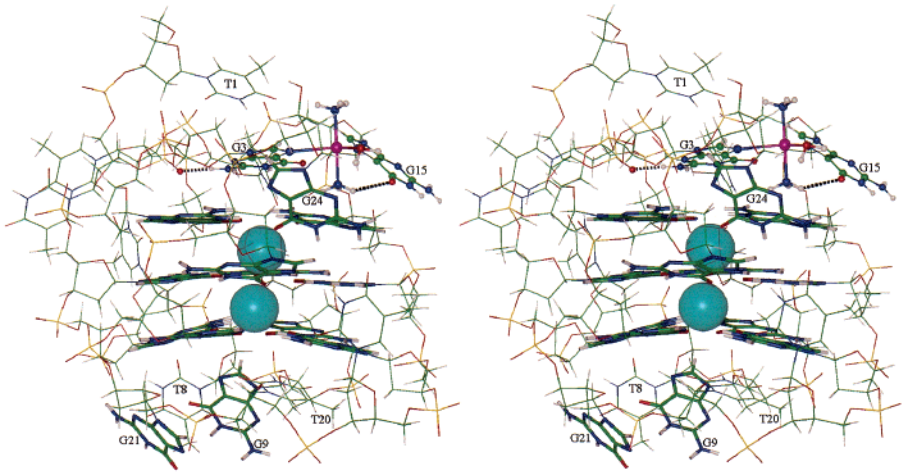

FIGURE 5: Structure **D**. Stereoview of the pentacoordinated state for the G3 chelation of the G15 monoadduct formed with **3**. The guanine bases are represented in "stick" format, and the size of the Na^+ cation represents its van der Waals radius. The energy of the minimized structure is $E = -755$ kcal·mol^{-1}. The hydrogen bonds G3(O1P)−G3(H21) and G15(O6)−Pt(N1ax) are represented by dashed lines. (Structure **E** for the G3 chelation of the G15 monoadduct of **2** is presented in Figure 4S of the Supporting Information.)

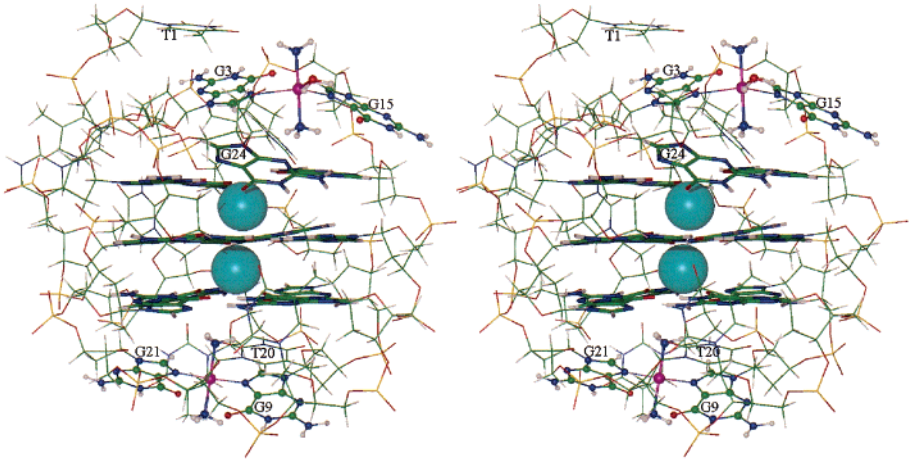

FIGURE 6: Structure **F**. Stereoview of the pentacoordinated state of the G3 chelation of the G15 monoadduct of **3**, occurring after formation of the G9-G21 chelate of **3**. The guanine bases are represented in "stick" format, and the size of the Na^+ cation represents its van der Waals radius. The energy of the minimized structure is $E = -775$ kcal·mol^{-1}.

because G3 is hindered by its stacking with T14 and is bound to one end cation, and also because both G21 and G24 are bound to the other end cation.

The G9-G24 cross-linking by complex **3** was only found together with the G3-G15 chelate (vide supra). This diadduct could not be accounted for by any of the previously proposed models **a** and **b** (Figure 1). Therefore, we proposed the schematic model **c** (Figure 1) and calculated structure **C**, which is 30 kcal·mol^{-1} less stable than **A** (Figure 2S Supporting Information).

To test the cross-linking pathways of folded $(T_2G_4)_4$ by complexes **2** or **3**, we calculated the pentacoordinated intermediates of the chelation reactions to occur on the first formed monoadducts (see Experimental Procedures and Figure 3S, Supporting Information). The rMD simulations involving dicationic platinum adducts all gave structures which retained only two sandwiched Na^+ between the G-quartets. Figure 5 represents the pentacoordinated intermediate **D** of the G3 chelation of the aqua monoadduct formed by **3** on G15 (the G3-G15 chelate is the single product of band 3.2, Figure 3). A similar analysis of the same cross-linking by **2** is presented in **E**, which is 25 kcal·mol^{-1} higher than the chelation path for **3** (Figure 4S, Supporting Information). The formation of the G9-G21 and G9-G24 cross-links with **3** was also examined (not shown). None of these chelations affected the stacking of the G-quartets.

To analyze the bis-cross-linking by **3**, at both ends of the G-quadruplex structure, we chose to first build the G9-G21 and G9-G24 *trans*-Pt$(NH_3)_2$ chelates because the platination by complex **1** occurred faster on G9 than on G15. We then calculated the pentacoordinated intermediates of the G3-G15 chelation. For the G9-G21/G3-G15 bis-chelate, the second cross-link can be made without any distortion of the quadruplex structure **F** (Figure 6). Whereas a perturbation of the stacking of the G-quartets was already induced by the G24 to G9 first chelation, it was amplified by the second G3 to G15 chelation (not shown).

DISCUSSION

Three platinum complexes have been used to study the structure of the telomeric sequence $(T_2G_4)_4$ in the presence of 50 mM Li^+, Na^+, or K^+.

Among the complexes $[Pt(NH_3)_3(H_2O)]^{2+}$ (**1**), *cis*-$[Pt(NH_3)_2(H_2O)_2]^{2+}$ (**2**), and *trans*-$[Pt(NH_3)_2(H_2O)_2]^{2+}$ (**3**), the latter reacted 1 order of magnitude slower than the other

two. Such a lower reactivity of **3** has already been reported with nucleotides (*42*, *43*) and can be essentially assigned to the lower pK_a of its first aqua ligand (4.35) compared to those of **2** and **1** (respectively 5.4 and 5.9), increasing the proportion of the less-reactive monocationic aqua-hydroxo species in solution (*44*, *45*).

The major results from our work are the following:

(1) $(T_2G_4)_4$ Adopts a Similar Type of Folding in the Presence of Li^+, Na^+, and K^+. Despite different migrations on the nondenaturing gel (Figure 1S, Supporting Information), these folded structures give the same platination pattern with the monofunctional complex **1** which binds to the same four guanines G3, G9, G15, and G21. This agrees with a common structure of type **a** initially proposed by Williamson et al. (*22*) (Figure 1) in which these four guanines are not involved in G-quartets. Their relatives reactivities: G9 > G15 ≫ G3 > G21, can be interpreted by their relative accessibilities depending on their stacking with the neighboring bases and on their binding of the end cations as shown by our rMD simulations (structure **A**, Figure 2). Such a cation binding is expected to be tighter with K^+ than with Na^+ or Li^+, which can also explain the slower platination reactions in K^+ medium. A K^+ binding within the loops of d(GGGCT$_4$GGGC) has been proposed from NMR studies (*46*).

(2) The Stability of the Quadruplex Structure Depends on the Nature of the Cation in the Decreasing Order $K^+ > Na^+ \gg Li^+$. The reaction of $(T_2G_4)_4$ with a very large excess of **1** (750:1) showed that Li^+ did not protect any of the 16 guanines from platination, Na^+ protected the central core of the 3 G-quartets, and K^+ gave the same platination pattern as with the 3:1 ratio. These differences reflect the influence of the cation on the stability of the quadruplex folding. The $K^+ > Na^+ \gg Li^+$ stability order agrees with thermodynamic data reported by several authors (*6*, *26*, *47*).

*(3) The Quadruplex Structure **A** Simulated by Restrained Molecular Dynamics Calculations Gives a Detailed Description of the Folded Form of $(T_2G_4)_4$.* It confirms the schematic model **a** (*22*) and accounts for all the platination data by **1**. The interpretation of the latter does not require the presence of the folded form **b** (*24*) as far as no G6 or G24 platinated adducts were found within our detection limit. It is noteworthy that $(T_2G_4)_4$ bearing either the G9-monoadduct or the G9, G15-diadduct of **1** exhibits a nondenaturing gel migration similar to that of the unplatinated $(T_2G_4)_4$, suggesting a similar folding of the three oligonucleotides.

(4) The Bifunctional Complexes cis- and trans-$[Pt(NH_3)_2(H_2O)_2]^{2+}$ Bind to the Same Guanines as Those Platinated by $[Pt(NH_3)_3(H_2O)]^{2+}$ and Are Able to Cross-Link Both Ends of the Quadruplex Structure. The cross-linking reactions are controlled by several factors: the stability of the quadruplex structure, the proximity between the chelating guanines and those bearing the monoadducts, the stereochemistry of the chelation due to the cis or trans geometry of the complex, the competition between chelation and further platination, and the hindrance of chelation due to end-cation binding. The formation of a G3-G15 cross-link was observed with both the cis and trans complexes **2** and **3**, respectively, in Na^+ and in both Na^+ and K^+. This shows that after release of the end cation, structure **A** has enough mobility to accommodate chelation of the monoadducts of both isomers. However, our rMD simulations of the pentacoordinated intermediates of the G3-G15 chelation suggest that it is easier with **3** than with **2** by 25 kcal·mol^{-1}. Our experiments showed that **2** gave more multiplatination than **3** (Figure 3) and that whereas the G3-G15 chelate of *trans*-Pt$(NH_3)_2$ was isolated as a single adduct, the same chelate of *cis*-Pt$(NH_3)_2$ was simultaneously present with monoadducts on G9 and G21 (or G24). Similarly, neither the G9-G21 nor the G9-G24 pure chelates of **2** were characterized, and the corresponding chelates of **3** were identified but only in association with other adducts. An rMD simulation of the pentacoordinated intermediate of the G21-G9 chelation (on the G9 monoadduct) showed that it was easier with **3** than with **2** by 30 kcal·mol^{-1} ($E = -764$ and -735 kcal·mol^{-1}, respectively) (not shown). All these data, together with our calculations, show that it is easier to cross-link both ends of the quadruplex with the trans complex **3** than with the cis **2** and that the latter, reacting faster, favors multiplatination at the expense of chelation.

*(5) Among the Three Quadruplex Structures **A**, **B**, and **C** Proposed for $(T_2G_4)_4$, **A** Presents the Best Stacking of the G-Quartets and Leads to Cross-Linking Reactions That Do Not Perturb This Stacking.* The "front diagonal loop" of **B** and **C**, schematically represented on **b** and **c** (Figure 1), is associated with a perturbation of the overall stacking (Figure 2S, Supporting Information). This is reflected by a -30 kcal·mol^{-1} difference between E_A and E_C. A comparable difference is found between the pentacoordinated intermediates of the G3-G15 chelation occurring either after formation of the G9-G21 cross-link on **A** (**F**, Figure 6) or after formation of the G9-G24 cross-link on **C** (not shown). Comparing structures **A** and **F** shows that it is possible to cross-link the quadruplex at both ends without perturbing the overall structure and quartet stacking.

CONCLUSION

The monofunctional complex $[Pt(NH_3)_3(H_2O)]^{2+}$ **1** is a good tool to analyze the folded structures of oligonucleotides containing telomeric sequences. The adducts of complex **1** formed upon reaction with the available guanines of $(T_2G_4)_4$ (40−90% yield) revealed the following: (i) the telomeric sequence adopts the same type of folding in the presence of Li^+, Na^+, or K^+; (ii) the decreasing stability of the quadruplex structure is in the order $K^+ > Na^+ \gg Li^+$; (iii) the decreasing order of reactivity of the guanines in the folded structure is G9 > G15 ≫ G3 > G21; (iv) the platination data agree with the schematic model of quadruplex structure proposed by Williamson et al. and are all interpreted with the structure simulated by our rMD calculations.

Among the cis and trans bifunctional complexes $[Pt(NH_3)_2(H_2O)_2]^{2+}$, the trans isomer **3** is the best suited to cross-link the free guanines at both ends of the quadruplex structure **A** and give isolable adducts. (i) The best results were obtained in K^+-containing solution (ca. 5% yield for each adduct); (ii) a cross-linked adduct between G3 and G15 at the "top end" of structure **A** was isolated as a single product; (iii) a bis-cross-link was also formed at both ends of structure **A** between G3-G15 and G9-G21; (iv) for these mono- and bis-cross-linking reactions, our rMD calculations revealed no perturbation of the quadruplex structures.

Telomerase interaction with mono- and bis-cross-linked G-quadruplex structures is being investigated for this and other telomeric sequences.

ACKNOWLEDGMENT

We thank Dr. Jírí Kozelka for the ab initio calculations of the pentacoordinated intermediates and for his comments concerning the molecular modeling. EC support for scientific exchanges within the COST D8/0009/97 program is acknowledged.

SUPPORTING INFORMATION AVAILABLE

Four figures showing nondenaturing gel electrophoresis of $(T_2G_4)_4$ in the presence of Li^+, Na^+, and K^+ (Figure 1S), a stereoview of structure **C** of $(T_2G_4)_4$ in Na^+ solution (Figure 2S), molecular models of the pentacoordinated intermediates *cis*- and *trans*-$[Pt(NH_3)_2(Gua)_2(H_2O)]^{2+}$ (Figure 3S), and structure **E** (Figure 4S) (5 pages). This material is available free of charge via the Internet at http://pubs.acs.org.

REFERENCES

1. Blackburn, E. H., and Greider, C. W. (1995) *Telomeres*, Cold Spring Harbor Press, Cold Spring Harbor, NY.
2. Daniels, G. A., and Lieber, M. R. (1995) *Proc. Natl. Acad. Sci. U.S.A. 92*, 5625−5629.
3. Fry, M., and Loeb, L. A. (1994) *Proc. Natl. Acad. Sci. U.S.A. 91*, 4950−4954.
4. Simonsson, T., Pecinka, P., and Kubista, M. (1998) *Nucleic Acids Res. 26*, 1167−1172.
5. Williamson, J. R. (1994) *Annu. Rev. Biophys. Biomol. Struct. 23*, 703−730.
6. Hud, N. V., Smith, F. W., Anet, F. A., and Feigon, J. (1996) *Biochemistry 35*, 15383−15390.
7. Patel, D. J., Bouaziz, S., Kettani, A., and Wang, Y. (1999) in *Oxford Handbook of Nucleic Acid Structure*, pp 389−453, Oxford University Press Inc., New York.
8. Shay, J. W., and Wright, W. E. (1996) *Curr. Opin. Oncol. 8*, 66−71.
9. Herbert, B.-S., Pitts, A. E., Baker, S. I., Hamilton, S. E., Wright, W. E., Shay, J. W., and Corey, D. R. (1999) *Proc. Natl. Acad. Sci. U.S.A. 96*, 14276−14281.
10. Greider, C. W. (1996) *Annu. Rev. Biochem. 65*, 337−365.
11. Zahler, A. M., Williamson, J. R., Cech, T. R., and Prescott, D. M. (1991) *Nature 350*, 718−720.
12. Fletcher, T. M., Sun, D., Salazar, M., and Hurley, L. H. (1998) *Biochemistry 37*, 5536−5541.
13. Sun, D., Thompson, B., Cathers, B. E., Salazar, M., Kerwin, S. M., Trent, J. O., Jenkins, T. C., Neidle, S., and Hurley, L. H. (1997) *J. Med. Chem. 40*, 2113−2116.
14. Fedoroff, O. Y., Salazar, M., Han, H., Chemeris, V. V., Kerwin, S. M., and Hurley, L. H. (1998) *Biochemistry 37*, 12367−12374.
15. Perry, P. J., Gowan, S. M., Reszka, A. P., Polucci, P., Jenkins, T. C., Kelland, L. R., and Neidle, S. (1998) *J. Med. Chem. 41*, 3253−3260.
16. Wheelhouse, R. T., Sun, D., Han, H., Han, F. X., and Hurley, H. H. (1998) *J. Am. Chem. Soc. 120*, 3261−3262.
17. Raymond, E., Sun, D., Chen, S. F., Windle, B., and Von Hoff, D. D. (1996) *Curr. Opin. Biotechnol. 7*, 583−591.
18. Mergny, J. L., and Helene, C. (1998) *Nat. Med. 4*, 1366−1367.
19. Burger, A. M., Double, J. A., and Newell, D. R. (1997) *Eur. J. Cancer 33*, 638−644.
20. Ishibashi, T., and Lippard, S. J. (1998) *Proc. Natl. Acad. Sci. U.S.A. 95*, 4219−4223.
21. Lepre, C. A., and Lippard, S. J. (1990) *Nucleic Acids Mol. Biol. 4*, 9−38.
22. Williamson, J. R., Raghuraman, M. K., and Cech, T. R. (1989) *Cell 59*, 871−880.
23. Henderson, E. R., Moore, M., and Malcolm, B. A. (1990) *Biochemistry 29*, 732−737.
24. Wang, Y., and Patel, D. J. (1994) *Structure 2*, 1141−1156.
25. Reeder, F., Kozelka, J., and Chottard, J. C. (1996) *Inorg. Chem. 35*, 1413−1415.
26. Hardin, C. C., Henderson, E., Watson, T., and Prosser, J. K. (1991) *Biochemistry 30*, 4460−4472.
27. Maxam, A. H., and Gilbert, W. (1980) *Methods Enzymol. 65*, 499−560.
28. Comess, K. M., Costello, C. E., and Lippard, S. J. (1990) *Biochemistry 29*, 2102−2110.
29. Lemaire, M. A., Schwartz, A., Rahmouni, A. R., and Leng, M. (1991) *Proc. Natl. Acad. Sci. U.S.A. 88*, 1982−1985.
30. Pearlman, D., Case, D. A., Caldwell, J. W., Ross, W. S., Cheatham, T. E., Ferguson, D. M., Seibel, G. L., Singh, U. C., Weiner, P. K., and Kollman, P. A. (1995) Amber 4.1, University of California, San Francisco.
31. Cheatham, T. E., Cieplack, I. P., and Kollman, P. A. (1999) *J. Biomol. Struct. Dyn. 4*, 845−862.
32. Herman, F., Kozelka, J., Stoven, V., Guittet, E., Girault, J. P., Huynh-Dinh, T., Igolen, J., Lallemand, J. Y., and Chottard, J. C. (1990) *Eur. J. Biochem. 194*, 119−133.
33. Chval, Z., and Síp, M. (1998) *J. Phys. Chem. 102*, 1659−1661.
34. Frisch, M. J., Trucks, G. W., Schlegel, H. B., Gill, P. M. W., Johnson, B. G., Robb, M. A., Cheeseman, J. R., Keith, T. A., Petersson, G. A., Montgomery, J. A., Raghavachari, K., Al-Laham, M. A., Zakrzewski, V. G., Ortiz, J. V., Foresman, J. B., Cioslowski, J., Stefanov, B. B., Nanayakkara, A., Challacombe, M., Peng, C. Y., Ayala, P. Y., Chen, W., Wong, M. W., Andres, J. L., Replogle, E. S., Gomperts, R., Martin, R. L., Fox, D. J., Binkley, J. S., Defrees, D. J., Baker, J., Stewart, J. P., Head-Gordon, M., Gonzalez, C., and Pople, J. A. (1995) Gaussian 94 revision C3, Gaussian, Inc., Pittsgurgh, PA.
35. Besler, B. H., Merz, K. M. J., and Kollman, P. A. (1990) *J. Comput. Chem. 11*, 431−439.
36. Simmerling, C., Elber, R., and Zhang, J. (1995) in *Modelling of Molecular Structure and Mechanisms* (Pullman, A., Ed.) pp 241−265, Kluwer, Dordrecht, The Netherlands.
37. Tuffery, P. (1995) *J. Mol. Graph. 13*, 67−72.
38. Basolo, F., and Pearson, R. G. (1967) in *Mechanism of Inorganic Reactions. A Study of Metal Complexes in Solution*, pp 351−453, J. Wiley & Sons Inc., New York, London, and Sydney.
39. Collman, J. P., Hegedus, L. S., Norton, J. R., and Frike Finke, R. G. F. (1987) in *Principles and Application of Organotransition Metal Chemistry*, p 242, University Science Books, Mill Valley, CA.
40. Dalke, A., Humphrey, W., and Ulrich, J. (1996) *VMD (Visual Molecular Dynamics), Version 1.2b1. Theoretical Biophysics Group*, University of Illinois and Beckman Institute, Urbana, IL.
41. Hirao, I., Nishimura, Y., Tagawa, Y., Watanabe, K., and Miura, K. (1992) *Nucleic Acids Res 20*, 3891−3896.
42. Arpalathi, J., Marjaana, M., and Mauristo, S. (1993) *Inorg. Chem. 32*, 3327−3332.
43. Mikola, M., Oksman, P., and Arpalahti, J. (1996) *J. Chem. Soc., Dalton Trans.*, 3101−3104.
44. Appleton, T. G., Bailey, A. J., Barnham, K. J., and Hall, J. R. (1992) *Inorg. Chem. 31*, 3077−3082.
45. Berners-Price, S. J., Frenkiel, T. A., Frey, U., Ranford, J. D., and Sadler, P. J. (1992) *J. Chem. Soc., Chem. Commun.*, 789−791.
46. Bouaziz, S., Kettani, A., and Patel, D. J. (1998) *J. Mol. Biol. 282*, 637−652.
47. Pilch, D. S., Plum, G. E., and Breslauer, K. J. (1995) *Curr. Opin. Struct. Biol. 5*, 334−342.

BI001565A